

Chemical Bonding State of Chlorine on Ag{100} as Determined by Angle-Resolved Secondary Ion Mass Spectrometry

Che-Chen Chang* (張哲政) and Chien-Hua Lung (龍健華)
Department of Chemistry, National Taiwan University, Taipei, Taiwan, R.O.C.

The power of the angle-resolved ion desorption technique for straightforward characterization of surfaces is demonstrated. The structural sensitivity of secondary ion desorption has led to a successful application of angle-resolved ion sputtering yield measurements to the determination of the Cl chemical bonding structure on the Ag{100} surface. Angular distributions of the sputtered Cl⁻ ions show that chlorine dissociates at the surface to yield a bonding state of atomic form at the room temperature. Both the polar and the azimuthal angle dependencies of the sputter intensity for Ag⁺ and Cl⁻ ions reveal that the Cl adatom is chemisorbed high above the topmost substrate layer of Ag atoms. At all Cl exposures, the Ag-Cl bond is oriented along the <100> azimuth with the adsorbate occupying a C₄ symmetry site, not an a-top, a bridge, or a high symmetry site. Shadow-cone enhanced ion desorption spectra show that the geometrical structure of the Cl chemisorbed surface changes slightly as the exposure is increased.

INTRODUCTION

The determination of the adsorbate geometry on solid surfaces is central to the understanding of the role of chlorine as a moderator¹ in the silver-catalyzed² heterogeneous selective oxidation of ethylene to ethylene oxide. To measure the adsorbate geometry, a number of surface spectroscopies have been developed, including low energy electron diffraction (LEED),³ scanning tunneling microscopy,⁴ surface extended x-ray absorption fine structure (SEXAFS),⁵ electron stimulated desorption,⁶ ion scattering spectrometry,^{7,8} and angle-resolved secondary ion mass spectrometry (SIMS).^{9,10} Among these techniques, the angle-resolved SIMS approach is chosen in this study since the underlying theory is simple and the sensitivity is high. Applications of this technique to the studies on the structural alterations associated with surface chemical reactions have proved highly successful.¹¹

This study is concerned mainly with the chemical bonding state of the chemisorbed Cl on a Ag{100} surface. It is known from LEED studies that at a coverage of more than ~0.4 monolayer (ML),¹² chlorine is chemisorbed at room temperature on the Ag{100} surface to form a Cl surface unit cell with its length on each side twice as large as that of the substrate Ag unit cell (so-called the Ag{100}-c(2×2)-Cl structure).¹³ The adsorption saturates at 0.5 ML.¹² Results of the surface structure analysis of Ag{100}-c(2×2)-Cl by LEED,¹⁴ angle-resolved ultraviolet photoelectron spectroscopy,¹⁵ He atom diffraction,¹⁶ SEXAFS,^{17,18} thermodynamic adsorption isotherms,¹⁹ and by SW-X α -SCF calculations²⁰ favor an adsorption geometry of Cl occu-

pying above the Ag substrate. However, in close agreement with angle-resolved photoemission data,²¹ results from the linear-combination-of-atomic-orbitals (LCAO) calculations^{22,23} favor a geometry, suggested by Rovida, et al.,¹³ in which the adsorbed Cl atoms (i.e., the Cl adatoms) and the Ag atoms from the substrate are roughly coplanar.

The potential of SIMS in characterizing subtle chemical bonding configurations on the surface is explored in the present study. The contradictory arguments about the bonding registry of Cl on Ag{100} at room temperature is re-examined using angle-resolved SIMS methods. The study also serves to explore the analytical capability of these surface-sensitive methods in differentiating surface geometrical structures of similar bonding symmetry. Our preliminary results²⁴ from an initial study of the c(2×2)-Cl overlayer on Ag{100} have shown that the sputtered Ag⁺ ions exhibit unique azimuthal angle distributions at different polar angles of detection, θ_a . The distribution is known to vary with the bonding structure and with the height of the atom above the surface.²⁵ Further, results from an angle-resolved SIMS method operated in the mode of shadow-cone enhanced secondary ion desorption indicates that the Ag-Cl bond-length is 2.60 ± 0.04 Å. This characterization approach has a surface sensitivity of about one monolayer.¹¹

The present study is aimed to explore at the atomic level the Cl bonding state on the surface after the Ag{100} surface is exposed to Cl molecules. It employs a detailed analysis of the angular dependence of the sputtered ion intensity for revealing significant chemical information about the reaction of chlorine with the surface. As the chlorine gas is allowed to react with the Ag crystal, it may chemisorb on

the surface as a molecule or decompose at some reactive sites to form adatoms. Because of the presence of a variety of active sites on the Ag{100} surface, the chemisorbed Cl species may bond on the surface at either a four-fold hollow site, a bridge site, or an a-top site. With the chemisorption geometry of Cl on the four-fold hollow site, the chlorine species resides inside an interaction potential well among four top-layer Ag atoms which are symmetrically positioned on the Ag{100} surface around a C_4 axis perpendicular to the surface. At this site, the Cl species may reside at the center of the hollow site (i.e., at the C_4 symmetry site) or off the center (i.e., at a high-symmetry site). Further, the size of the Cl species varies significantly with the amount of the charge it carries, with the radius of a fully negatively charged Cl ion being about twice as large as that of a neutral Cl atom. Thus, depending on the charge state of the Cl species on the surface, the chemisorbed Cl may reside high above the surface, occupy a top-layer interstitial site, or diffuse into the Ag substrate. It is also expected that following the chemisorption of Cl on the surface, a series of chemical reactions may take place such that the Cl species may erode the substrate, replace the top-layer Ag atoms, or form an overlayer above the substrate. Many of these bonding alternatives of Cl on Ag{100} have not been adequately examined and addressed before.

EXPERIMENTAL ASPECTS

All experiments are performed in a UHV angle-resolved scattering chamber that has been described in detail elsewhere.²⁶ The experimental conditions have also been described previously.¹⁰ Briefly the background pressure is about 2×10^{-10} torr. A 2–4 keV primary ion beam of 0.2–5 nA with a beam cross-section ≤ 2 mm² is focused on the target crystal. The sputtered species are filtered through a 90° energy analyzer before entering a quadrupole mass spectrometer. Both the energy analyzer and the mass spectrometer are located in a rotation platform which allows them to be positioned independently from the rest of the system. The experimental parameters are defined in Fig. 1a. In the azimuthal angle distribution, only high energy species of 20 ± 3 eV are collected to ensure that the resulting distribution reflects better the chemical bonding geometry of the surface.⁹ Angular resolution of the energy and mass analyzers is about $\pm 0.25^\circ$ (polar) or $\pm 2^\circ$ (azimuthal).

The Ag single crystal with a surface parallel to the {100} crystal plane is oriented by Laue diffraction to within 0.5° and mechanically polished to optical quality before being mounted on a copper sample holder. The surface is then

cleaned *in situ* by cycles of heating and ion bombardment (2 keV, $0.5 \mu\text{A}/\text{cm}^2$). Surface cleanliness is monitored by Auger electron spectroscopy and SIMS. Low energy electron diffraction is used to confirm the sample orientation and to ensure a (1×1) surface order. The sample is cleaned after about 90 minutes of data taking to ensure that the measurements are done on a fresh surface.

Orientation of the sample surface with respect to the ion beam is controlled by a goniometer which allows independent rotation of the crystal to any azimuthal angle and tilt of the sample to vary the polar angle of the incident ion beam, θ_i . The definitions of the angles employed in this work are shown in Fig. 1a. All polar angles will be given with respect to the surface normal. Chlorine is deposited on the surface by exposing the sample crystal at room temperature to the chlorine gas of 99.999% purity, purchased from Matheson. Exposures are determined by an uncorrected pressure reading, expressed in torr, from a nude Bayard-Alpert ionization gauge. An exposure of 1 langmuir (L) is equivalent to the encounter with the surface of a gaseous

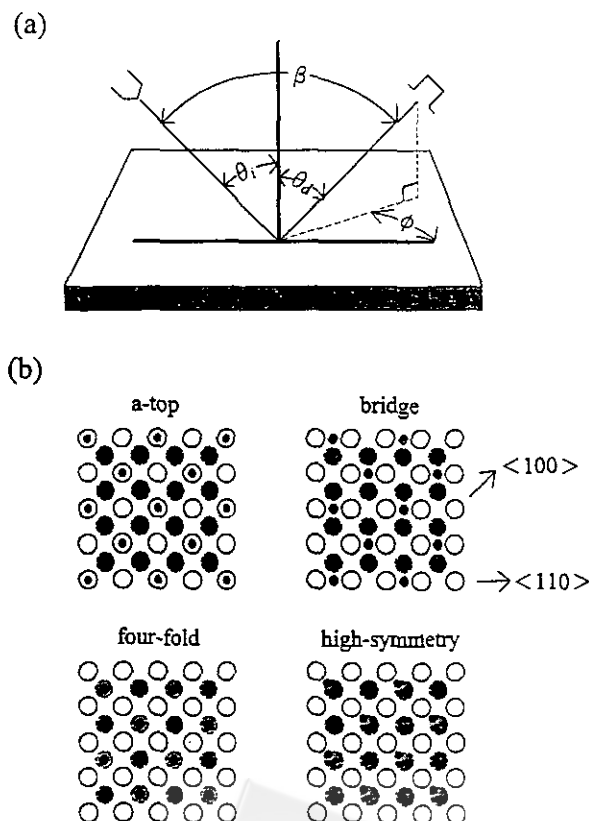


Fig. 1. (a) Parameter definitions for the experiment. (b) The Ag{100} surface with possible chemisorption sites. The open circle represents the top layer Ag atom, the hatched circle the second layer Ag atom, and the solid circle the Cl adsorbate.

molecule at a partial pressure of 1×10^{-6} torr in one second. In this study, the Cl partial pressure used for dosing ranges from 5×10^{-9} to 5×10^{-8} torr and the exposing time from 100 to 500 seconds, depending on the amount of exposure to be studied.

RESULTS AND DISCUSSION

The dependence of the secondary ion yield on the azimuth of incidence at various Cl exposures is shown in Fig. 2-4 for Ag^+ ions ejected from a Cl covered Ag{100} surface. In these spectra, ions which are ejected with high kinetic energies of 20 ± 3 eV are detected. The higher energy particles generally leave early in the collision cascade before the nearby surface atomic arrangement is perturbed. Thus, they reflect better the registry of surface atoms.^{25,27-29} Both the image potential between the ejecting ion and its image charge in the substrate and the coulomb potential among adsorbates are also too small to affect the departing trajectories of the ions with high kinetic energies.

The secondary ion azimuthal anisotropy can be correlated with the geometrical structure of the surface.²⁵ As

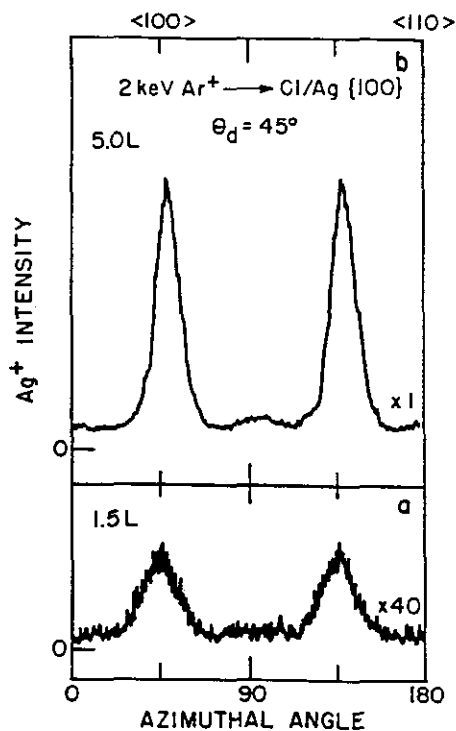


Fig. 2. Azimuthal angular distributions of Ag^+ ions from a Ag{100} surface exposed at room temperature to (a) 1.5 L, (b) 5.0 L of chlorine. The surface is bombarded by Ar^+ ions of 2 keV energy at an incident angle of normal to the surface. The sputtered particles are collected at $\theta_a = 45^\circ$.

shown in Figs. 2 and 3, minimum Ag^+ ion intensities are found to always appear along $\langle 110 \rangle$ azimuths, which correspond to the directions of close-packed rows of atoms in the surface plane of the substrate. Ions emitted along these directions are obstructed on their way out of the surface except at small values of θ_a . On the other hand, the intensity profile of the sputtered Ag^+ ion is sensitive to the Cl exposure. At a Cl exposure of 1.5 L, the Ag^+ ion intensity arises to its maximum along the $\langle 100 \rangle$ direction for $\theta_a = 45^\circ$ (see Fig. 2a). It has been reported²⁵ that the ejecting trajectory of the substrate ions from an adsorbate-covered surface is governed by a strong channeling effect exerted on the departing substrate ions by their nearest-neighbor substrate atoms and by those adsorbates along the ion departing trajectory. Further, the LEED pattern obtained at this coverage is similar to the one obtained from a clean surface, indicating that the adsorbates are randomly distributed on surface reaction sites at this exposure. Inspection of a model crystallite of Ag{100} shows that, in addition to some high-symmetry adsorption sites, there are three possible reaction sites which are of low symmetry. They are the a-top site, the bridge site, and the four-fold hollow site (see Fig. 1b). A random adsorption of Cl on the bridge site should cause the sputtered Ag^+ ion to depart from the surface preferably along a $\langle 110 \rangle$ direction of a deep interaction potential well. Similarly, occupation

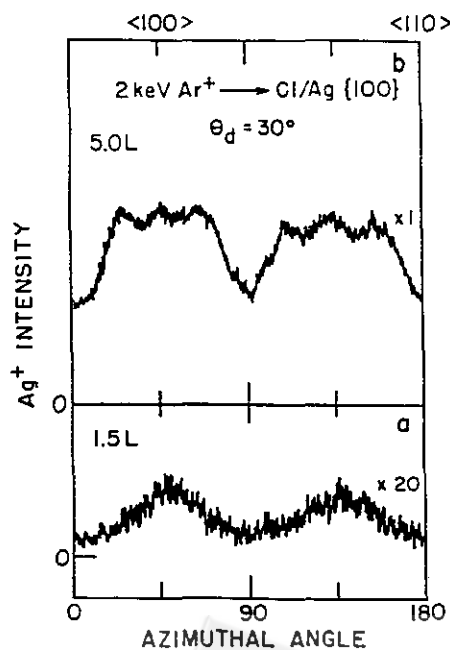


Fig. 3. Azimuthal angular distributions of Ag^+ ions from a Ag{100} surface exposed at room temperature to (a) 1.5 L, (b) 5.0 L of chlorine. The surface is bombarded by Ar^+ ions of 2 keV energy at an incident angle of normal to the surface. The sputtered particles are collected at $\theta_a = 30^\circ$.

of Cl on the a-top site should block the departing Ag^+ ion from proceeding along the $\langle 100 \rangle$ direction and cause the measured peak position of the sputtered ions to be shifted off the $\langle 100 \rangle$ azimuth. The observation of a maximum Ag^+ ion intensity along the $\langle 100 \rangle$ azimuth thus rules out the possibility of Cl adsorption at this coverage on either the bridge or the a-top site.

At a Cl exposure of 5.0 L, a LEED pattern of $c(2 \times 2)$ structure is observed. The adsorption symmetry revealed in the azimuthal angle spectrum of the sputtered Ag^+ ions (see Fig. 2b) at this exposure is the same as that predicted by the $c(2 \times 2)$ LEED structure.^{27,28} As shown in the spectrum, the Ag^+ ion intensity also arises to its peak along the $\langle 100 \rangle$ direction. It indicates that at this exposure the Cl adsorbate also bonds in the surface on a site other than the a-top or the bridge site. Because of the similarity of the azimuthal angle distributions at the 1.5 L and 5.0 L exposures of the Ag^+ ions sputtered from the surface, the adsorption site of Cl at these two exposures is believed to be identical. Further, the symmetry of the sputter intensity in these spectra indicates that the Cl adsorbate does not occupy a high-symmetry site on the surface but a C_4 symmetry site. However, these distributions do not reveal exactly how Cl is adsorbed. It may be either above the surface on the hollow site¹⁴⁻²⁰ or coplanar with the Ag atom of the substrate.^{13,21-23}

The relative height of the Cl adsorbate to the position

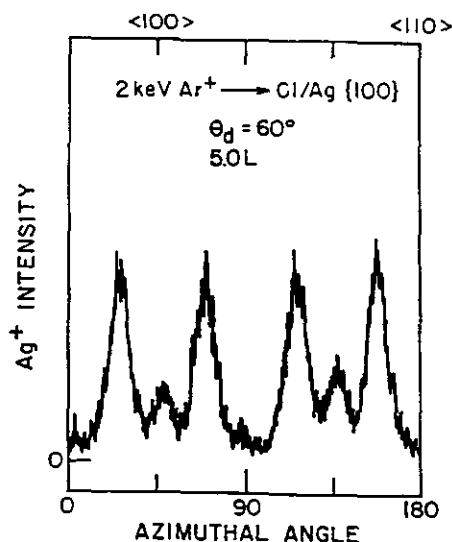


Fig. 4. Azimuthal angular distribution of Ag^+ ions from a $\text{Ag}(100)$ surface exposed at room temperature to 5.0 L of chlorine. The surface is bombarded by Ar^+ ions of 2 keV energy at an incident angle of normal to the surface. The sputtered particles are collected at $\theta_d = 60^\circ$. The amplification factor of the Ag^+ intensity relative to the intensity scale used in Fig. 2b is 20.

of the Ag atom on the surface may be understood by studying the azimuthal dependence of the Ag^+ ion yield at $\theta_a = 30^\circ$. At this small polar angle of detection from the surface normal, the interaction of the outgoing Ag^+ ion from the topmost layer and its nearest-neighbor atoms in the same layer is very weak. The ejecting ions are expected to be less obstructed at $\theta_a = 30^\circ$ than at $\theta_a = 45^\circ$. It should result in a smaller azimuthal anisotropy.^{26,29} However, a strong anisotropy is still observed in our spectrum for the Ag^+ ion ejected at $\theta_a = 30^\circ$ from a $\text{Ag}\{100\}$ - $c(2 \times 2)$ -Cl surface (see Fig. 3b). The prominent feature in this spectrum is an ion intensity profile of three yield maxima centered at the $\langle 100 \rangle$ azimuth. This feature can only be explained by the fact that the Cl adsorbate is located above the topmost layer of Ag atoms and that Cl occupies every other rows of C_4 symmetry sites along the $\langle 100 \rangle$ direction. The triplet feature observed in fig. 3b is due to two different ion ejection mechanisms. The Ag ions ejected along the direction perpendicular to the line connecting adjacent Cl adsorbates contribute to the sputter intensity at the $\langle 100 \rangle$ azimuth. However, the Ag ions ejected parallel to the Cl-Cl bond are partially blocked at $\theta_a = 30^\circ$ by the overlayer Cl atoms. It results in maximum intensities at azimuthal angles about 20° off the $\langle 100 \rangle$ direction. The blocking effect is insignificant at low exposures, since most of the four-fold hollow sites on the surface are unoccupied at this level of coverage. Thus, instead of exhibiting a sputter intensity profile with multiple maxima along the $\langle 100 \rangle$ azimuth, the Ag^+ ion distribution at the low Cl exposure (e.g., 1.5 L) exhibit a similar azimuthal angle spectrum (see Fig. 3a) at $\theta_a = 30^\circ$ as that obtained at $\theta_a = 45^\circ$. The observed chemical bonding of Cl above the $\text{Ag}(100)$ surface is in agreement with the results obtained by surface extended x-ray absorption fine structure spectrometry.¹⁷

The Ag^+ ions ejected from a $c(2 \times 2)$ AgCl -like mixed layer surface will not result in an azimuthal distribution with a peak intensity of multiple maxima. On this surface, the chemisorbed Cl and the epitaxial Ag atoms occupy every other rows of four-fold hollow sites along the $\langle 100 \rangle$ crystallographic direction. Further, most of the ejected atoms are believed to originate from the top surface layer,³⁰ especially in the case where the top layer has a close-packed structure. The angular anisotropy of the Ag^+ ions ejecting from substrate layers underneath the AgCl -like dense overlayer does not contribute significantly to the observed Ag^+ ion azimuthal distribution. Thus, for Cl to be chemisorbed coplanar with the Ag atom on the surface, the Ag^+ ions emitted from the AgCl overlayer may leave the surface relatively free of the blocking effect. Due to the presence of the Cl adsorbate nearby on the surface, the ejecting Ag^+ ions should be somewhat driven to move along the $\langle 100 \rangle$ azimuth and

give rise to a sputter intensity of a single maximum along this direction. This prediction is in disagreement with what is shown in Fig. 3b. Other possible overlayer geometries of the Cl adsorbate, such as the a-top and the two-fold bridge structures,^{14,19,31} will result in Ag⁺ ion azimuthal distributions at $\theta_a = 30^\circ$ vastly different to that shown in Fig. 3b.

A large azimuthal anisotropy is observed for Ag⁺ ions sputtered from a Ag{100}-c(2×2)-Cl surface at a polar angle of detection from the surface normal. As shown in Fig. 4, sputtering of Ag⁺ ions at $\theta_a = 60^\circ$ gives rise to sharp peaks of intensity at about 20° off on the both sides of the <100> azimuth. With Cl adsorbates positioned at the C₄ symmetry site above the surface, the Ag⁺ ion emitted at the large polar angle along the <100> direction experiences a strong repulsive interaction with the overlayer Cl adsorbate. The interaction almost completely blocks the emitted ion from proceeding along the <100> azimuth. However, there exists a narrow open channel between a Cl adsorbate and two top-layer Ag atoms, one being located at the <110> direction relative to the emitted atom and the other at <100>, which allows an ejecting top-layer Ag⁺ ion to take off from the surface. Since there is a narrow channel at about 20° off the <100> direction on each side, two sharp peaks of sputter intensity are thus obtained along each <100> azimuth.

The sputter intensity of the Cl⁻ ions ejected from a Cl covered Ag{100} surface is further studied as a function of

the azimuthal angle of detection. As shown in Fig. 5, the Cl⁻ ions are found to preferentially eject along the <100> azimuth at a Cl exposure of 0.5 L. The preferential direction of ejection can be understood if one considers the collision cascade initiated by the incident energetic particle.³² Both the results from experimental measurements and that from molecular dynamics simulations have shown^{9,28} that at low coverages of adsorbates, the direction of ejection of the adsorbed species is governed by the trajectory of the topmost layer substrate atoms, not by the presence of surface channels. Since the topmost layer Ag atoms tend to eject along the <100> direction, as revealed in Fig. 2a, these atoms transfer their momentum to the adsorbates if they are located along the path of the emitting Ag atoms. The fact that at $\theta_a = 45^\circ$ a high sputter yield of Cl⁻ ions is observed at the <100> azimuth (Fig. 5) indicates that at 0.5 L the Ag-Cl bond is oriented along the <100> direction and the Cl adsorbate is above the topmost layer Ag atoms.

The dependence upon the azimuthal detection angle of the sputter intensity of the Cl⁻ ions ejected from a Cl covered Ag{100} surface is found to be very sensitive to the Cl exposure. As shown in Figs. 5 and 6a, the sputter intensity of

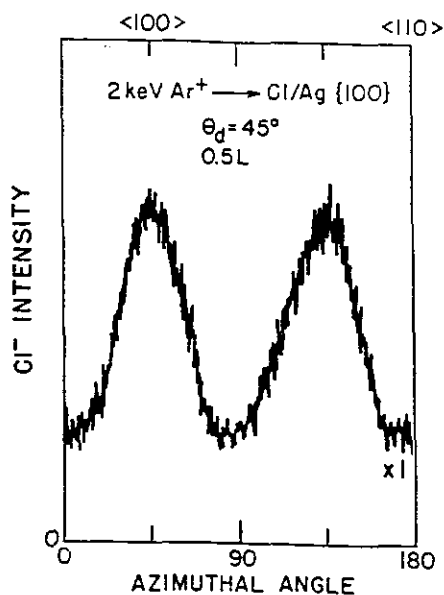


Fig. 5. Azimuthal angular distribution of Cl⁻ ions from a Ag{100} surface exposed at room temperature to 0.5 L of chlorine. The surface is bombarded by Ar⁺ ions of 2 keV energy at an incident angle of normal to the surface. The sputtered particles are collected at $\theta_d = 45^\circ$.

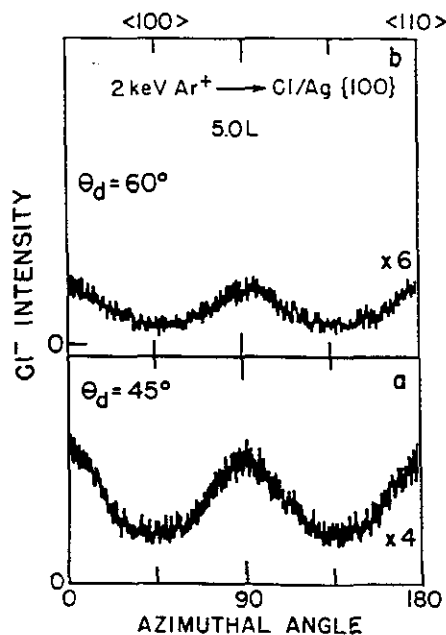


Fig. 6. Azimuthal angular distributions of Cl⁻ ions from a Ag{100} surface exposed at room temperature to 5.0 L of chlorine. The surface is bombarded by Ar⁺ ions of 2 keV energy at an incident angle of normal to the surface. The sputtered particles are collected at (a) $\theta_d = 45^\circ$, (b) $\theta_d = 60^\circ$. The amplification factor of the Cl⁻ intensity shown for each distribution is relative to the intensity scale used in Fig. 5.

the ejected Cl⁻ ions along the <100> direction changes from a maximum to a minimum value as the exposure is increased from 0.5 L to 5.0 L. The shift of the peak position of the sputter intensity from the <100> to the <110> azimuth results from a change of the dominant ejection mechanism of Cl⁻ ions as the Cl coverage on the surface is increased. It is expected that at the saturation exposure of 5.0 L¹² where a c(2×2) LEED structure is observed, the surface channeling effect exerted by nearby Cl adsorbates dominates the Cl⁻ ion ejection process. The open surface channel formed by the atoms nearest to the ejecting Cl species is along the <110> direction for Cl chemisorbed on the C₄ symmetry site. On the other hand, the epitaxial AgCl-like surface has open surface channels along <100> azimuths. The observation of minimum intensities along <100> azimuths and maximum intensities along <110> directions for Cl⁻ ions sputtered from a Ag{100}-c(2×2)-Cl surface confirms that at room temperature Cl prefers to chemisorb above the Ag surface at the C₄ symmetry site at the saturation exposure.

In sharp contrast to what is observed for Ag⁺ ions sputtered from the Cl covered Ag{100} surface, the Cl⁻ ions exhibit an azimuthal angle distribution of four-fold symmetry at $\theta_a = 60^\circ$. The distribution is similar to the one obtained for Cl⁻ ions at $\theta_a = 45^\circ$, except that the dependence of the sputter intensity upon the azimuthal angle of detection is weak. Because of the identical atomic arrangement of Cl and Ag atoms in the AgCl-like mixed-layer adsorbate structure, the Cl⁻ and Ag⁺ ions are expected to exhibit similar azimuthal angle dependence if they are ejected from a AgCl-like epitaxial layer. The spectrum of four-fold symmetry, instead of a spectral feature of the sputter intensity maximized at 20° off the <100> azimuth on each side, observed in Fig. 6b for Cl⁻ ions emitted at $\theta_a = 60^\circ$ thus excludes again the possibility of Cl forming an epitaxial AgCl-like structure on the surface when 5.0 L of it is exposed to Ag{100}. Since the Cl adsorbate binds above the surface, the interaction between the departing Cl species at $\theta_a = 60^\circ$ and the underlying Ag atoms is too weak to result in an angular distribution similar to that observed in Fig. 4.³¹

A single sputter intensity maximum observed at the <110> direction in the azimuthal distribution of Cl⁻ ions also reveals that chemisorption of Cl on the surface is in the atomic form. If chemisorption causes Cl to occupy the four-fold hollow site of the Ag{100} surface in the diatomic form and with the Cl-Cl bond oriented somewhat perpendicular to the surface, one would expect to observe at $\theta_a = 60^\circ$ an azimuthal distribution of multiple intensity maxima along the <110> azimuth for the Cl⁻ ion which ejects from the Cl atom closer to the surface. The multiplicity of the sputter intensity would be due to the same ejection mechanism as the one

that leads to the intensity peak of multiple maxima observed in Figs. 3b and 4. If chemisorption gives rise to an admolecule with the Cl-Cl bond oriented somewhat parallel to the surface, the bond would most possibly be arranged either above the Ag-Ag bond along the <100> direction or somewhat above the bridge site along the <110> direction. Because of the directional force exerted by the surface channels, each Cl atom of the admolecule in either case would each contribute to the azimuthal spectrum at $\theta_a = 60^\circ$ an independent set of two sputter intensity maxima in the angular range of 0° to 180°. The two sets of intensity maxima do not overlap with each other since these two Cl atoms of the admolecule would be displaced from the center position above the hollow site. These predictions are not in agreement with what shown in Fig. 6b. Thus, Cl is chemisorbed on the surface in the atomic form.

The bonding geometry of the adsorbate on the surface is also reflected in the polar angle distribution.^{25,29,31,33} This distribution is sensitive to the take-off positions and the effective sizes of the ejecting species.^{25,31} Due to the blocking effect at large angles of detection, the polar angle distribution for species ejected originally from the top surface layer has a maximum sputter intensity at an angle close to the surface normal. As shown in Fig. 7, the Cl⁻ ion sputter intensity

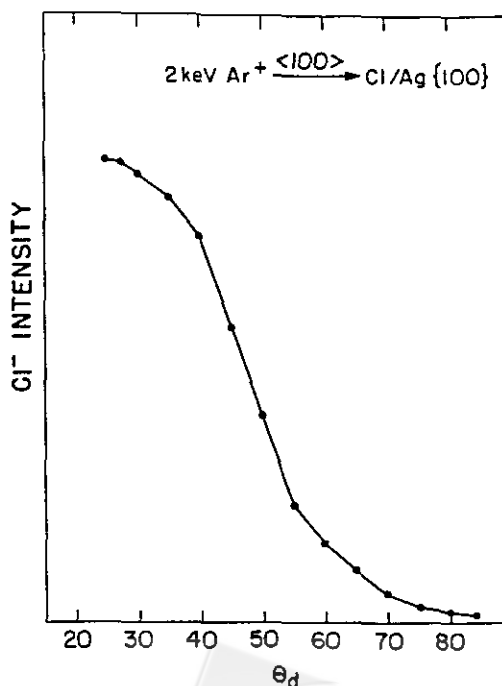


Fig. 7. Dependence upon the polar detection angle along the <100> azimuth of the secondary ion yield of Cl⁻ from a Ag{100} surface covered at room temperature by about 0.5 monolayer of chlorine. The surface is bombarded by Ar⁺ ions of 2 keV energy at an incident angle of normal to the surface.

exhibits a polar angle dependence with the maximum yield occurring at an angle close to the surface normal for Cl chemisorbed on Ag{100} at the saturation exposure. We note that the sputter yield at $\theta_a = 0^\circ$ cannot be measured with our experimental configuration, since in our experiments the primary particles are allowed to impinge on the surface at normal incidence.

Similar polar angle distributions should be observed for the Ag^+ and Cl^- ions ejected from a AgCl-like mixed layer surface. However, the Ag^+ ions exhibit a polar angle dependence, shown in Fig. 8, which has very low sputter intensity at detection angles close to the surface normal. As the polar angle of detection is increased from $\theta_a = 0^\circ$, the Ag^+ ion yield increases first and then decreases. The maximum yield occurs at a polar angle of about 48° . The presence of the maximum Ag^+ ion yield at a large polar angle of detection indicates²⁹ that Ag atoms do not bind in the top surface layer. The polar angle dependence of the sputter intensity for both Ag^+ and Cl^- ions thus reveals that the Cl adsorbate is chemisorbed high above the topmost substrate layer of Ag atoms.

With shadow-cone enhanced SIMS,^{10,34,35} the decision between the bonding structure of a simple Cl overlayer and

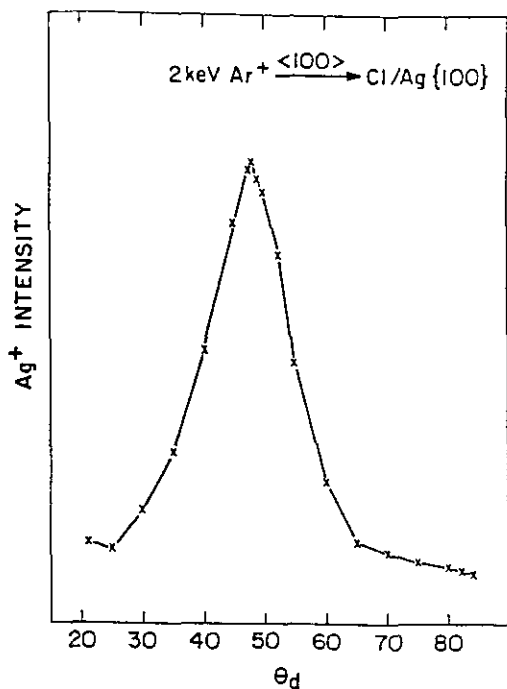


Fig. 8. Dependence upon the polar detection angle along the $\langle 100 \rangle$ azimuth of the secondary ion yield of Ag^+ from a Ag{100} surface covered at room temperature by about 0.5 monolayer of chlorine. The surface is bombarded by Ar^+ ions of 2 keV energy at an incident angle of normal to the surface.

that of the AgCl-like mixed layer becomes quite straightforward. The shadow-cone enhanced SIMS technique has a surface sensitivity of about one monolayer.¹⁰ It has been reported that the maximum secondary ion intensity, due to shadow-cone enhanced ion desorption,³⁴ is dependent on the angle of incidence only. It is independent of the angle of detection or the angle between the ion gun and the detector, β , for surface species ejected from the topmost atomic layer. For the case of the adatom-covered surface, it is expected that only the ions ejected from the adlayer exhibit the β independency. Shown in Fig. 9 are incident angle distributions of Cl^- ions along $\langle 100 \rangle$ azimuth at $\beta = 25^\circ$ and 35° for 3 keV Ar^+ ions incident on a Ag{100}-c(2x2)-Cl surface. The intensity of Cl^- ions sputtered from the surface is seen to vary as the angle of incidence θ_i is changed from 0° to 90° . Due to the ion-focusing effect at the tail of the shadow cone,³⁵ the intensity rises to peaks at $\theta_i = 28.5^\circ$ and 64.0° , as θ_i is increased. The position of these intensity peaks in Fig. 9 is found to be independent of the angle β . The changes as a function of β in the relative intensity of the peak at $\theta_i = 28.5^\circ$ to that at $\theta_i = 64.0^\circ$ arise from a blocking of desorbing

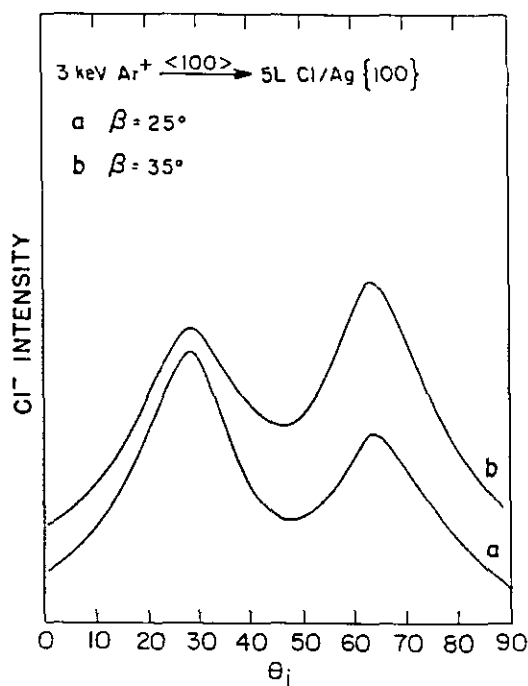


Fig. 9. Incident angle distributions along the $\langle 100 \rangle$ azimuth of Cl^- ions from a Ag{100} surface covered at room temperature by 0.5 monolayer of chlorine. The angle between the ion gun and the detector is selected as (a) 25° , (b) 35° . The surface is bombarded by Ar^+ ions of 3 keV energy at an incident angle of normal to the surface. The spectra shown here are also taken at room temperature.

Cl species by other surface atoms, which occurs only at large values of θ_i and small values of β .³⁴

However, both the shadow-cone effect and the channeling effect dominate the Ag^+ ion incident angle distribution. As shown in Fig. 10, the distributions exhibit intensity maxima at different angles of incidence for different angles β . In addition to the sputter intensity maxima obtained due to shadow-cone enhanced ion desorption, as those seen in the Cl⁻ ion angular distributions in Fig. 9, other peaks at $\theta_i \sim 71^\circ$ for $\beta = 25^\circ$ and at $\theta_i \sim 18^\circ$ and 63° for $\beta = 35^\circ$ are also observed in the Ag^+ ion distributions. Calculation of the shadow-cone shape using a Thomas-Fermi-Moliere potential³⁶ indicates that these new peaks may arise from both the shadow-cone effect and the sputtering process in which the ejected Ag^+ ions are channeled out of the surface. If one examines a three-dimensional model of the $\text{Ag}\{100\}$ surface, channels defined by both the substrate and the surface atoms are observed along the $\langle 100 \rangle$ azimuth. There are two alternating sets of nonequivalent atomic planes along this azimuth perpendicular to the $\text{Ag}\{100\}$ -c(2 \times 2)-Cl surface. One set of the planes is terminated by Cl adatoms on the surface

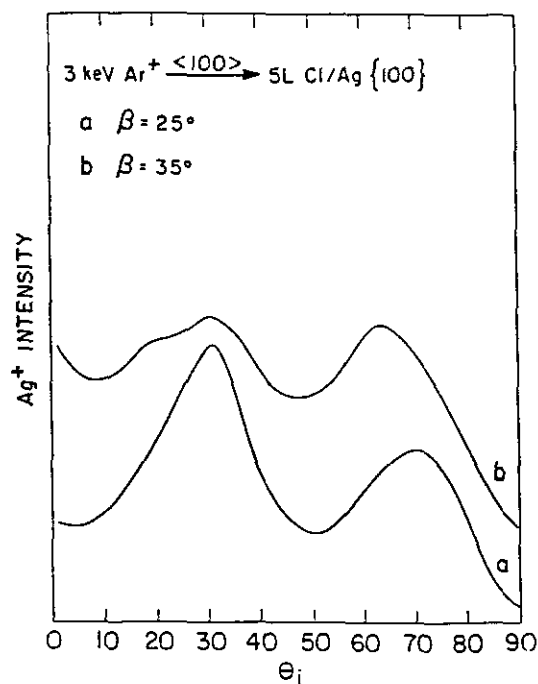


Fig. 10. Incident angle distributions along the $\langle 100 \rangle$ azimuth of Ag^+ ions from a $\text{Ag}\{100\}$ surface covered at room temperature by 0.5 monolayer of chlorine. The angle between the ion gun and the detector is selected as (a) 25° , (b) 35° . The surface is bombarded by Ar^+ ions of 3 keV energy at an incident angle of normal to the surface. The spectra shown here are also taken at room temperature.

and the ejection direction of Ag^+ ions are governed by the two Cl adatoms at the open end of the channel. The other set of the planes is terminated by the topmost substrate layer Ag atoms. The ejection direction of Ag^+ ions from this plane is governed by the size of the hollow site formed by four Cl adatoms in the overlayer and/or four Ag atoms in the topmost substrate layer. The directional effect of these channels in the Ag- and Cl-terminated planes contributes to the observed Ag^+ ion angular distributions in different degrees at different angles β . It thus results in the β -dependent spectral features in Fig. 10. The β -dependency of the Ag^+ ion angular distribution and the β -independency of the Cl⁻ ion distribution indicate that the chlorine atomic plane is above the silver surface plane, which means that Cl chemisorbs as a simple overlayer on the Ag surface. We note that the directional effect of the channels in the $\text{Ag}\{100\}$ -c(2 \times 2)-Cl surface is not as strong as the one observed in the $\text{Ag}\{110\}$ -c(4 \times 2)-Cl³⁴ system. Chlorine adsorption saturates at a lower coverage of ~ 0.5 ML^{13,37,38} on the $\text{Ag}\{100\}$ surface, compared with a Cl saturation coverage of 0.75 to 1.0 ML on the $\text{Ag}\{110\}$ -c(4 \times 2)-Cl surface.^{39,41} No shadow-cone enhanced desorption of Ag^+ ions from the $\text{Ag}\{110\}$ -c(4 \times 2)-Cl surface can be observed in the Ag^+ ion incident ion distribution.³⁴

Changes in the chemical bonding structure may occur when the Cl exposure on the $\text{Ag}\{100\}$ surface is increased. Shown in Fig. 11 is an azimuthal angle distribution of Ag^+ ions sputtered from a $\text{Ag}\{100\}$ surface exposed to 25 L of chlorine. The distribution has an intensity peak of three maxima at $\theta_a = 30^\circ$. Similar to that obtained for Ag^+ ions sputtered from the surface exposed to 5 L of chlorine, the peak is centered at the $\langle 100 \rangle$ azimuth. However, the yield of the Ag^+ ions ejected along the direction perpendicular to the chemical bond between two overlayer Cl atoms along the $\langle 100 \rangle$ direction, which contributes to the observed maximum intensity at the $\langle 100 \rangle$ direction, is increased as the exposure is increased from 5 L to 25 L. This indicates that the height of the Cl adatom above the Ag surface may be decreased due to the depolarization of the Cl adsorbates at increasing coverages. This observation is in agreement with the results obtained from a study about the Cl reaction chemistry on the $\text{Ag}\{110\}$ surface.³⁴

The decrease of the Ag-Cl bond length reflects a change of the charge distribution in the bond as the reaction between Cl and Ag proceeds on the surface. For example, the radius of a neutral Cl atom has a radius of 0.99 Å, whereas a fully charged Cl⁻ ion has a radius of 1.81 Å. Since the ionic or covalent characteristics of the adsorbate controls the promoting role of Cl in the catalytic conversion of ethylene to ethylene oxide,⁴² the catalytic activity of the Cl-

covered Ag surface may change accordingly. This may explain why Cl, which is highly negatively charged at low coverages and slightly charged at high coverages, acts as a promoter for ethylene epoxidation in small amounts and as a toxic agent when its amount is increased. The decrease of the amount of charge on the Cl atom at high exposures is due to an increase in interaction of surface Ag-Cl dipoles.

CONCLUSIONS

The specific experimental arrangements presented here provide unique and straightforward approach to determine the chemical bonding of foreign species on the surface. As illustrated in the study of the chemisorption of a catalytic moderator on surface, the arrangements allow SIMS to be operated as an angle-resolved technique. The inherent versatility of the angle-resolved experiment makes possible the studies of the surface structural alteration during a chemical reaction. The operation theory is simple and the sensitivity for surface characterization is high.

As shown in this study, the angle-resolved ion desorption technique may provide detailed information about the identity of the bonding adsorbates, the site of the chemisorption, the relative height of the adsorbed species, and the interaction of adsorbates with the substrate. It may be used in

differentiating surface structures of similar symmetry on the adsorbate registry. Except that the angle of detection has to be variable, the equipment requirement of this type of spectrometric measurements is no more than what is usually found in an ordinary surface analysis system, i.e., an ion gun, a mass spectrometer and a sample manipulator with two rotational degrees of freedom.

Chlorine saturated Ag{100} exhibits a $c(2 \times 2)$ LEED structure. At room temperature, it forms a chemisorbed overlayer with Cl atoms bonding in the C_4 symmetry sites above the topmost Ag layer. Similar to the chemical activity of halides on the Ag{110} surface, this chemisorbed Cl overlayer may facilitate ethylene epoxidation on Ag{100} surfaces. On the other hand, the Ag{111} surface, on which a pseudo-AgCl{111} epitaxial layer is believed to form,⁴³ has very low catalytic activity for ethylene oxide formation.⁴⁴ It is known that the ionic or covalent characteristics of the chemisorbed overlayer may determine the reactivity of the surface.⁴² The characteristics of the overlayer is governed by the specific adsorbate, the chemical state of the adsorbate, the identity of the substrate, the reaction temperature, and the adsorbate coverage. The inertness of the Ag{111} surface for catalysis may be associated with its high surface atomic density and its small corrugation of the reaction potential surface. Studies are underway to determine why the Ag{100} surface has lower catalytic activity than the Ag{110} surface.

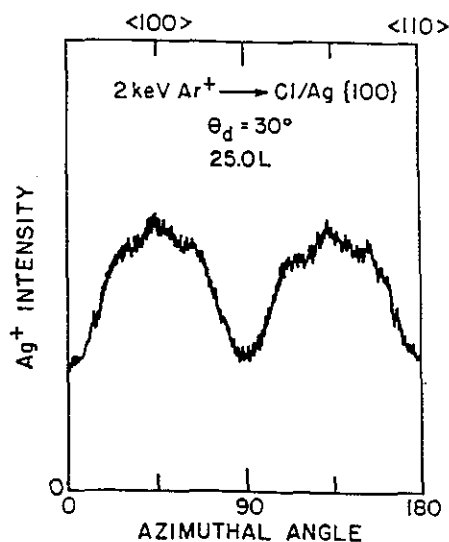


Fig. 11. Azimuthal angular distribution of Ag^+ ions from a Ag{100} surface exposed at room temperature to 25.0 L of chlorine. The surface is bombarded by Ar^+ ions of 2 keV energy at an incident angle of normal to the surface. The sputtered particles are collected at $\theta_d = 30^\circ$. The spectrum is shown here with the same intensity scale as the one used in Fig. 3b.

ACKNOWLEDGMENT

We would like to gratefully acknowledge discussions with N. Winograd. In addition, the financial support of the ROC National Science Council is gratefully acknowledged.

Received November 27, 1995.

Key Words

Angle-resolved secondary ion mass spectrometry; Shadow-cone enhanced ion desorption; Catalysis; Ethylene epoxidation.

REFERENCES

1. Voge, H.; Adams, C. *Adv. Catal.* **1967**, *17*, 151.
2. Verykios, X. E.; Stein, F. P.; Coughin, R. W. *Catalysis Rev. Sci. Eng.* **1980**, *22*, 197.
3. Kruger, B.; Benndorf, C. *Surface Sci.* **1986**, *178*, 704.

4. Stroscio, J. A.; Feenstra, R. M.; Fein, A. P. *Phys. Rev. Lett.* **1987**, *58*, 1668.
5. Citrin, P. H.; Hamann, D. R.; Mattheiss, L. F.; Rowe, J. E. *Phys. Rev. Lett.* **1982**, *49*, 1712.
6. Madey, T. E.; Yates, Jr., J. T. *Surface Sci.* **1977**, *63*, 203.
7. Yarmoff, J. A.; Cyr, D. M.; Huang, J. H.; Kim, S.; Williams, R. S. *Phys. Rev.* **1986**, *B33*, 3856.
8. Heiland, W.; Taglauer, E. *Surface Sci.* **1977**, *68*, 96.
9. Winograd, N. *Springer series in Chem. Phys.* **1983**, *35*, 403.
10. Chang, C.-C.; Malafsky, G.; Winograd, N. *J. Vac. Sci. Technol.* **1987**, *A5*, 981.
11. Chang, C.-C.; Ph.D. Thesis, The Pennsylvania State University, **1987**.
12. Taylor, D. E.; Williams, E. D.; Park, R. L.; Bartelt, N. C.; Einstein, T. L. *Phys. Rev.* **1985**, *B32*, 4653.
13. Rovida, G.; Pratesi, F. *Surf. Sci.* **1975**, *51*, 270.
14. Zanazzi, E.; Jona, F.; Jepsen, D. W.; Marcus, P. M. *Phys. Rev.* **1976**, *B14*, 432.
15. Bartels, E.; Goldmann, A. *Solid State Communications* **1982**, *44*, 1419.
16. Cardillo, M. J.; Becker, G. E.; Hamann, D. R.; Serri, J. A.; Whitman, L.; Mattheiss, L. F. *Phys. Rev.* **1983**, *B28*, 494.
17. Lamble, G.; King, D. A. *Phil. Trans. R. Soc. Lond.* **1986**, *A318*, 203.
18. Citrin, P. H.; Hamann, D. R.; Mattheiss, L. F.; Rowe, J. E. *Phys. Rev. Lett.* **1982**, *49*, 1712.
19. Tu, Y.-Y.; Blakely, J. M. *Surf. Sci.* **1979**, *85*, 276.
20. Tian, Z.; Zhang, K.; Xie, X. *Surf. Sci.* **1985**, *163*, 1.
21. Weeks, S. P.; Rowe, J. E. *Solid State Communications* **1978**, *27*, 885.
22. Greenside, H. S.; Hamann, D. R. *Phys. Rev.* **1981**, *B23*, 4879.
23. Hamann, D. R.; Mattheiss, L. F.; Greenside, H. S. *Phys. Rev.* **1981**, *B24*, 6151.
24. Chang, C.-C.; Winograd, N. *Surf. Sci.* **1990**, *230* 27.
25. Winograd, N. *Springer Series in Chem. Phys.* **1983**, *35*, 403.
26. Gibbs, R. A.; Winograd, N. *Rev. Sci. Instrum.* **1981**, *52*, 1148.
27. Holland, S. P.; Garrison, B. J.; Winograd, N. *Phys. Rev. Lett.* **1979**, *43*, 220.
28. Holland, S. P.; Garrison, B. J.; Winograd, N. *Phys. Rev. Lett.* **1980**, *44*, 756.
29. Gibbs, R. A.; Holland, S. P.; Foley, K. E.; Garrison, B. J.; Winograd, N. *J. Chem. Phys.* **1982**, *76*, 684.
30. Harrison, Jr., D. E.; Kelly, P. W.; Garrison, B. J.; Winograd, N. *Surface Sci.* **1978**, *76*, 311.
31. Kapur, S.; Garrison, B. J. *J. Chem. Phys.* **1981**, *75*, 445.
32. Chang, C.-C. *Phys. Rev.* **1993**, *B48*, 12399.
33. Moon, D. W.; Winograd, N.; Garrison, B. J. *Chem. Phys. Lett.* **1985**, *114*, 237.
34. Chang, C.-C.; Winograd, N. *Phys. Rev.* **1989**, *B39*, 3467.
35. Chang, C.-C. *J. Formosan Sci.* **1995**, *48*, 7.
36. Torrens, T. M. "interatomic Potentials" Academic Press: New York, **1972**.
37. Kitson, M.; Lambert, R. M. *Surface Sci.* **1980**, *100*, 368.
38. Weeks, S. P.; Rowe, J. E. *J. Vac. Sci. Technol.* **1979**, *16*, 470.
39. Campbell, C. T.; Paffett, M. T. *Appl. Surface Sci.* **1984**, *19*, 28.
40. Bowker, M.; Waugh, K. C. *Surf. Sci.* **1985**, *155*, 1.
41. Briggs, D.; Marbrow, R. A.; Lambert, R. M. *Chem. Phys. Lett.* **1978**, *53*, 462.
42. Kleinherbers, K. K.; Janssen, E.; Goldmann, A.; Saalfeld, H. *Surf. Sci.* **1989**, *215*, 394.
43. Bowker, M.; Waugh, K. C. *Surf. Sci.* **1983**, *134*, 639.
44. Kummer, J. T. *J. Phys. Chem.* **1956**, *60*, 666.

